THE EFFECT OF ULTRA-THIN GRAPHITE ON THE MORPHOLOGY AND PHYSICAL PROPERTIES OF THERMOPLASTIC POLYURETHANE ELASTOMER COMPOSITES

Olivia Menes[a], Manuela Cano[b], Adolfo Benedito[a], Enrique Giménez[c], Pere Castell[d],

Wolfgang K. Maser[b], Ana M. Benito[b*]

[a]Materials_Research_Group, AIMPLAS, Instituto Tecnológico del Plástico, C/Gustave

Eiffel 4, E-46980 Paterna, Valencia (Spain)

[b]Department of Chemical Processes and Nanotechnology, Instituto de Carboquímica,

ICB-CSIC, C/Miguel Luesma Castán 4, E-50018 Zaragoza (Spain)

[c]Instituto de Tecnología de Materiales. Universidad Politécnica de Valencia, E-46022

Valencia (Spain)

[d]NANOZAR S L , Miguel Luesma Castán 4, E-50018 Zaragoza (Spain).

Abstract

Composites of thermoplastic polyurethane (TPU) and ultra-thin graphite (UTG) with

concentrations ranging from 0.5 to 3 wt% were prepared using a solution compounding

strategy. Substantial reinforcing effects with increased loadings are achieved. Compared

to neat TPU, values for storage modulus and shear viscosity are enhanced by 300 % and

150 %, respectively, for UTG concentrations of 3 wt%. Additionally, an enhancement

of thermal properties is accomplished. The crystallization temperature and thermal

stability increased by 30 ºC and 10 ºC, respectively, compared to neat TPU.

Furthermore, the use of oxidized UTG (UTGO) with its added functional oxygen

*Corresponding author. Tel.: +34 976 73 39 77; Fax: +34 976 73 33 18 (A.M. Benito).
E-mail addresses: omenes@aimplas.es (O. Menes), enrique.gimenez@mcm.upv.es (E.
Giménez), p.castell@nanozar.com (P. Castell), abenito@icb.csic.es (A.M. Benito).

groups suggests the presence of chemical interactions between UTG and TPU, which

additionally impact on the thermal properties of the corresponding composites.

Controlling the oxidation degree, thus offers further possibilities to obtain composites

with tailored properties. The presented approach is straightforward, leads to

homogeneous TPU-UTG composites with improved materials properties and is

especially suitable for commercial UTG materials and further up-scaled production.

Keywords: A. Nano composites, A. Functional composites, A. Polymers, A. Graphite

B. Thermomechanical properties

1. INTRODUCTION

Fillers are important to enhance the properties of polymers and can therefore be used for

the development of a new generation of composite materials with improved or new

functionalities [1]. In the last few decades, carbon-based nanomaterials, especially

carbon nanotubes have attracted great attention as nanofiller material [2]. Transferring

their exceptional electrical, thermal and mechanical properties to polymer matrices

leads to substantial multifunctional property enhancement, achieved at much lower

loading fractions than polymer composites with conventional micron-scale fillers [2, 3].

Graphene [4, 5], a single atomic layer of graphite, is a direct parent of carbon nanotubes

with equal if not superior performance, and thus considered as the ultimate carbon

nanofiller material [6]. The fact that graphene can be easily fabricated by different kinds

of exfoliation methods applied to inexpensive graphite even at larger scales and already

is commercially offered by various companies has renewed enthusiasm in the field of

polymer nanocomposite research [7]. Although commercial graphene produced by

exfoliation of graphite at industrial scale frequently is not fully exfoliated, this type of

graphene material, probably better described as ultra-thin graphite (UTG), retains its

importance as nanofiller for achieving improved performance and price advantages,

essential for new applications of polymers.

A polymer of great technological interest is thermoplastic polyurethane. It is one of the

most versatile materials for applications that demand high flexibility and elasticity [8,

9]. However, this polymer shows low mechanical strength and poor thermal stability

hampering its use in high-temperature applications. The incorporation of carbon

nanotubes [10-15] and nanoclays [16-18] has lead to significant improvements of these

polymer characteristics. First publications on graphene-based materials (graphene,

functionalized graphene, graphene oxide) also report on reinforcing effects in TPU [19-

25]. Various compounding approaches were taken: Melt mixing [25], solution mixing

[20-25], and *in-situ* polymerization [19, 25]. From an industrial point of view, the most

economically viable method is melt mixing. However, it is prone to re-aggregation of

graphene and thermal degradation of the TPU matrix [25]. On the other hand, highest

degree of dispersion is achieved by *in-situ* polymerization, followed by solution mixing

[25]. While *in-situ* polymerization if based on the use of polymer precursors, solution

mixing is the approach of choice when it comes to the use of already prefabricated TPU

matrices, especially those available from shelf.

In this work we describe the effect of commercial UTG materials on the physical

properties in TPU. To this end, TPU composites with different amounts of UTG were

prepared by solution compounding followed by subsequent coagulation process.

Morphology, structure, thermal and mechanical properties were probed by scanning

electron microscopy, X-ray diffraction, infrared and Raman spectroscopy, differential

scanning calorimetry, thermal gravimetric analysis, dynamic mechanical analysis and

rheological measurements. Increasing the amount of UTG in TPU leads to significant

enhancement of the storage modules up to 300 % and the viscosity up to 150 %
compared to neat TPU. Crystallization temperature and thermal stability increased by
30 ºC and 10 ºC, respectively. Furthermore, the use of oxidized UTG material (UTGO)
leads to chemical interactions between filler and the matrix, positively affecting thermal
and processing behavior. The applied approach is straightforward, suitable for
commercially available UTG and TPU materials, and leads to reinforced TPU-UTG
composites.

2. EXPERIMENTAL

2.1. Materials

Commercial grade, low density ultra-thin graphite (UTG) with a particle size of 1-1.5
µm and 15-20 nm of thickness was purchased from Avanzare S.L. (La Rioja, Spain).
Thermoplastic polyurethane elastomer PEARLTHANE® 11T85E (TPU) with a density
of 1.16g/cm^3 (at 20ºC) and a melt flow index of 10 g/10 min (190 °C, 21.6 kg) was
kindly provided by Merquinsa (Merquinsa, Barcelona, Spain) and used as received.
N,N-dimethylformamide (DMF; Scharlau, Barcelona S.L., Spain), methanol (MeOH;
Gilca S.C., Spain), H_2SO_4, 65% (Sigma-Aldrich Co.) and fuming HNO_3, 37% (Sigma-
Aldrich, Co.) were used as received.

2.2. Preparation of ultra-thin graphite oxide (UTGO)

Commercial UTG material was refluxed in a mixture of HNO_3 and H_2SO_4 3M (1/3 v/v)
for 24 h at 110 °C. The resulting material was filtered and washed with distilled water
until pH was neutral. Subsequently, the residue was dried under vacuum overnight at 80
°C. The commercial (UTG) and modified UTG materials (UTGO) were quantitatively
analyzed by titration to determine the COOH content on their surface [26]. In a typical

experiment, 100 mg of UTGO were dispersed into a 15 ml solution of 0,1 N NaOH,

bath sonicated for 30 min, and then stirred for 2 days at room temperature to allow the

graphite material to equilibrate with the NaOH solution. The obtained dispersion was

filtered under vacuum and the filtrate titrated with a 15 ml solution of 0.1N HCl to

determine the excess of NaOH present in the filtrate and therefore the concentration of

COOH groups on the materials. Concentration of carboxylic groups of UTG and UTGO

materials amounts to 6 mmol/g and 12 mmol/g, respectively.

2.3. Preparation of TPU composites

Different TPU-UTG composites with increased UTG loadings were prepared. Samples

were labeled as TPU, TPU-UTG0.5, TPU-UTG1, TPU-UTG2.5, and TPU-UTG3 for a

UTG content of 0, 0.5, 1, 2.5, and 3 wt.% respectively. A TPU-UTGO2.5 composite

with a load of 2.5 wt.% of UTGO was also prepared. In a typical experiment 3 g of TPU

were completely dissolved in 30 ml of DMF at 35 °C. On the other hand, the required

quantity of UTG or UTGO was dispersed in 25 mL of DMF and sonicated in an

ultrasound bath for 3 h to obtain homogeneous dispersion of both materials.

Subsequently, the UTG dispersion was added dropwise to the TPU solution, and the

mixture was stirred for 10 more min in order to get a homogeneous solution. Finally,

the mixture was slowly poured into 250 ml of MeOH and the precipitated TPU-UTG(O)

composites were washed several times with MeOH. The resulting material was dried

overnight at 65 °C in a vacuum oven. For neat TPU, the polymer was dissolved in the

total volume of DMF (55 mL) following the same preparation procedure in absence of

UTG.

2.4. Characterization

The morphology of the UTG starting material was examined by scanning electron microscopy (SEM) with a Hitachi S3400N microscope. The polymer-based samples were fractured, and the fractured surfaces were studied by field emission scanning electron microscopy (FE-SEM) with a JEOL JSM-7001F. The samples for FE-SEM were previously sputtered with platinum and afterwards with a conductive wire of colloidal Ag.

ATR-FTIR measurements were performed on a Perkin-Elmer System 2000 FTIR spectrometer incorporating an Attenuated Total Reflectance system (ATR). The spectra were recorded in the range from 500 to 4000 cm^{-1}.

Raman spectra were recorded with a Horiba Jobin Yvon HR800 UV spectrometer using an excitation wavelength of 532 nm. Scans were recorded in the range from 500 to 3000 cm^{-1}.

Powder X-ray diffraction (XRD) measurements were carried out at room temperature on a Bruker D8 Advance diffractometer using a Cu K$_\alpha$ X-ray radiation.

Differential scanning calorimetry (DSC) experiments were performed in a Mettler DSC-823e equipment at a scan rate of ± 20 °C·min^{-1} over a temperature range of -60 to 300 °C under a nitrogen flow of 100 mL/min. Indium was used as standard for the temperature and heat flow calibration. Different scans of dynamic heating at a rate of 10 and 20 °C/min were performed using a standard 100 μL aluminum pan containing 17 mg on average weight. A heating from room temperature up to 200 °C was applied at a rate of 20 °C/min to eliminate the processing thermal history of the samples. Subsequently, the samples were cooled to -60 °C at 20 °C/min to observe the crystallization transitions, and finally reheated up to 300 °C at 10 °C/min to analyze the melting behavior.

Thermogravimetric analyses were carried out using a Setaram Setsys Evolution 16/18.

The measurements were made from 20 °C to 900 °C at a heating rate of 10 °C/min

under N_2 atmosphere (100 mL/min) in order to evaluate the effect on TPU degradation.

Dynamic mechanical analysis (DMA) tests were carried out on a TA Instruments DMA

2980 equipment with a 3 point-bending mode applying at a heating rate of 3 °C/min in

the interval of -60 to 220 ºC, a frequency of 1Hz, a strain amplitude of 20 μm and a

preload of 0.01N. For this purpose, composite test specimens of 35 mm x 13 mm x 1.5

mm in size were prepared by a compression process at 180 °C applying a pressure of 2

metric tons for 10 min.

Rheological properties were measured using a rotational Rheometer AR-G2 TA

Instruments. Shear viscosities were tested by means of parallel plate geometry with 25

mm diameter and 1000 mm gap under nitrogen atmosphere. The temperature applied

was 190 °C and the shear rates ranged from 0,001 s^{-1} to 100 s^{-1}.

3. RESULTS AND DISCUSSION

3.1 UTG and UTGO materials

Morphology and structure of UTG was characterized by SEM and XRD techniques.

SEM micrograph (Figure 1a) reveals a flake-like morphology with lateral flake sizes

between hundreds and thousands of nanometers, and variable thickness ranging from a

few tens to a few hundreds of nanometers. X-Ray diffractograms (Figure 1b) present the

characteristic intense (002) diffraction peak at $2\theta=26.5°$ that corresponds to well-

ordered graphite interlayer distance of 3.35 nm. In case of the UTGO material, the (002)

peak becomes slightly broader, indicative for a lower graphitic structure.

Although no essential morphological and structural differences between UTG and

UTGO are detected, oxidation of UTG was verified by FTIR analysis (Figure 1c). UTG

7

material shows the characteristic bands at 1577, 2850 and 2910 cm^{-1} related to C=C and

C(sp^{2} aromatic)-H symmetric and asymmetric modes, respectively. The acid treated

UTGO exhibited an additional band appearing at 1728 cm^{-1} corresponding to C=O

stretching vibration of carboxyl groups incorporated during the acidic treatment,

therefore confirming its effective oxidation, in agreement with the titration results.

Raman spectra of the UTG, and UTGO materials (Figure 1d) show the characteristic

features typically observed for graphene-based materials, namely the D, G, and 2D

bands located at 1354, 1573, and 2700 cm^{-1}, respectively [27]. After the acid treatment,

the Raman intensity of the D band, related to disorder of the in-plane graphene

structure, increased with respect to the G band, associated with tangential C-C bond

stretching vibrations, thus clearly indicating that the structure of the UTG material has

been altered upon the oxidation treatment. The I_D/I_G ratio increased from 0.084 to 0.64

for the UTG and UTGO material, respectively, thus evidencing that the acid treatment

has introduced a high level of defects in UTG, which may serve as possible interaction

sites once incorporated into the TPU matrix.

3.2 Composite materials

Composites exhibit a relatively smooth and homogeneous fracture surface (Figure 2a).

The presence of UTG above 2.5 wt.% confers the composite a more platelet-like

morphology. However, no aggregates of graphite sheets were detected underlining the

good dispersion degree achieved by the applied solution mixing process, assisting to

overcome the strong tendency of graphene flakes to aggregate.

X-Ray diffractograms of the composite materials are presented in Figure (2b). TPU

itself exhibits a broad diffraction peak ranging from 18 to 23° and centered at 20.8° that

can be assigned to polycaprolactone (PCL) segment indicating a low degree of

crystallinity of the polymer. The X-Ray diffractograms of all the composite materials

reveal a superposition of both TPU and UTG features. Although weak, the presence of

the (002) graphite peak at 26.5º is visible in all samples and thus reveals the successful

incorporation of graphite into the polymer matrix. Its relatively low intensity reflects its

low concentration in TPU. For UTGO composite, the (002) peak is slightly broader, as

expected for the starting UTGO material (see section 3.1). For all materials, X-Ray

diffractograms clearly prove that UTG materials not only were successfully

incorporated in the TPU matrix, but furthermore, no structural modification of both

components took place as a consequence of the applied solution mixing approach.

Possible interactions between UTG (UTGO) and the TPU polymer matrix were studied

by FTIR and Raman spectroscopy (Figure 3). The FTIR spectrum (Figure 3a) of TPU

displays the characteristic N-H stretch band of urethanes at 3328 cm^{-1}, and two strong

vibrations at 1728 and 1709 cm^{-1} assigned to free and hydrogen-bonded carbonyl

groups, respectively [28]. Additionally, a band at 1597 cm^{-1} is ascribed to N-H in plane

bending mode, and the peaks at 1531 cm^{-1} are associated to the combination of N-H out

of the plane bending and C-H stretching. Moreover, the stretching C-O, and C-O-C

bands are visible at 1165 cm^{-1} and at 1074 cm^{-1}, respectively. No significant changes of

the TPU bands are observed when UTG or UTGO is incorporated even at the highest

concentration. The only exception is a slight change of the position of the N-H stretch

band which gradually shifts from 3328 in neat TPU to 3334 cm^{-1} in the UTG and

UTGO composites which eventually might suggest the existence of chemical

interactions between UTG and the TPU polymer matrix.

More sensitive information on what concerns possible interactions is provided by

Raman spectroscopy (Figure 3b and c). In all the spectra, the characteristic vibration

bands of polyurethane such as ν(CH2) at 2930, ν(C=O) at 1736, ν(C=C) at 1620, δ (C-

H) at 1445, and ν(C-O) at 1090 cm^{-1} are observed [29]. These characteristic polymer

bands decrease in intensity with UTG content. However, no apparent shifts are detected

when UTG is present. On the contrary, the characteristic G-band, clearly visible in all

the composite spectra, is up-shifted up to 12 cm^{-1} with increasing UTG content,

suggesting interactions between TPU and UTG due to interfacial stress transfer [30].

Moreover, when UTGO was used, the resulting TPU-UTGO2.5 composite not only

exhibits similar up-shifts in the characteristic graphene-based bands but additionally

downshifts of relevant TPU bands such as ν(CH2) appear now at 2924, ν(C=C) at 1615,

δ (C-H) at 1440, and ν(C-O) at 1072 cm^{-1}. Therefore, the spectroscopic observations

may provide some slight hints for the formation of additional chemical interactions

between UTGO and TPU induced by the presence of oxygen functional groups and/or

additional disorder related defects on UTGO. These might offer further opportunities

for improved materials properties, as outlined in the following.

Dynamic mechanical analysis (DMA) provided insight into the influence of UTG on the

mechanical properties and molecular structure of the TPU-UTG composites. The

storage modulus E' and tan δ of TPU, TPU/UTG and TPU/UTGO composites as a

function of temperature are shown in Figure 4. From -40 to 0º C a steep decrease of the

storage modulus E' (Figure 4a), typical for enhanced chain mobility in the TPU matrix

upon transition through the glass transition temperature T_g, is observed [19]. Beyond 0

ºC a more gradual decrease of E' i.e. a more gradual increase in chain mobility is noted.

The presence of UTG in the TPU matrix leads to improved E' values which is even

more pronounced beyond T_g. At room temperature, the highest value of E', namely

105.20 MPa, is achieved for the composite containing 3 wt.% of UTG (Figure 4b). This

corresponds to an increase of approximately 300% with respect to the storage modulus

E' of 30.65 MPa found for neat TPU, and thus represents a substantial stiffening of the

TPU matrix. Please note, that the UTG concentration of 3 wt% does not necessarily represent the optimum loading fraction. Regarding the behavior of the composite containing UTGO, no difference is observed between TPU-UTG2.5 and TPU-UTGO2.5 at room temperature, indicating that the presence of functional groups in UTGO has no significant influence on the value of the storage modulus of the resulting composite. The tan δ peak (Figure 4c) is related to the soft segment dynamic glass transition temperature T_g [31]. The introduction of UTG resulted in a shift of T_g to higher temperatures. An increase of 6 °C for T_g is observable for composites containing 3 wt.% of UTG (Table 1). Most likely, the well-dispersed UTG restricts the molecular motion of the polymer chains and therefore leads to an increase in the values for T_g. This is even more significant for UTG loadings above 2.5 wt.%.

Rheological measurements exploring the variation of viscosity with shear rate as shown in Figure 5 provide further insight into the molecular structure of the composite materials. The viscosity decreased gradually with incrementing shear rates, indicating a non-Newtonian behavior due to the random orientation of the rigid molecular chains, typically observed in composite systems [32, 33]. However, at low shear rates between 0.001 and 0.01 s^{-1} a Newtonian plateau in which the viscosity does not depend on the shear rate is observed. Values of viscosity for the prepared composites in this range of deformation increased with the UTG content. Here the value of 16200 Pa·s for the TPU-UTG3 composite is 150 % higher than the one for the neat TPU (10565 Pa·s). On the other hand, the Newtonian plateau is shifted to lower shear rate as the percentage of UTG increases. The addition of UTG to TPU apparently leads to the formation of a weak three-dimensional UTG network that may remain intact at very low shear rates resulting in overall higher viscosity values for the composite materials indicative of a more solid-like behavior [33, 34]. These results are consistent with the increased storage

modulus E' observed in DMA tests and once again point out that the incorporation of

UTG and UTGO into the TPU matrix results in reinforced composites with improved

performance. As for the dynamic mechanical measurements the use of UTGO does not

have any significant effect on the rheological properties. Apparently, the overall degree

of oxidation and defects in UTGO, which leads to chemical interactions with the TPU

polymer matrix, is too small to influence at low UTGO concentrations on the motion of

the TPU chains and thus does not affect the storage modulus and viscosity.

Next the thermal properties of the composites were investigated Figure 6. From DSC

crystallization curve (Fig. 6a) it can be seen that neat TPU shows an exothermic peak

indicating the crystallization of the polymer at 70 °C. When UTG and UTGO are

incorporated into the polymer matrix a second exothermic peak evolves at higher

temperatures (100 °C). Its intensity increases with the content of UTG, suggesting that

UTG here acts as effective nucleating agent for the molten TPU chains. However,

despite the observed changes in the crystallization behavior, the overall crystallinity of

the polymer, as determined from the heat of fusion ΔH_m (Table 1), remains almost

constant in all the TPU-UTG composites, in agreement also with the observed XRD

results. Remarkably, in case of the composite containing 2.5 wt% of UTGO, the second

crystallization peak centered at 100 °C appears as the most intense one, pointing to a

strong interaction between UTGO and the TPU matrix, most likely related to the

presence of functional oxygen groups and defect sites in UTGO, as observed by Raman

spectroscopy. DSC melting curves (Figure 6b) and the derived values for the heat of

fusion ΔH_m, related to the melting of the hard segments of the TPU matrix, and the

melting temperature T_m provide additional information on the influence of UTG(O) on

crystallinity and crystal sizes in the composites. As can be seen from Table 1, the

presence of UTG in the different composites does not reveal significant differences in

12

the heat of fusion, thus indicating that the overall degree of crystallinity in the studied samples is not modified. However, the composite containing UTGO shows a completely different behavior. Here the heat of fusion ΔH_m is 50 % lower compared to neat TPU matrix underlining a substantial reduction of the overall degree of crystallinity of the resulting composite. Furthermore, in contrast to UTG, the melting temperature increased by 3 ºC with respect to the neat TPU polymer and is even 1.7 ºC higher than the corresponding TPU-UTG composite. This is indicative of slightly larger crystal sizes in the soft segment TPU domain [21] of the corresponding composite, most likely related to the presence of functional groups and defects on the UTGO surface. These interactions would enhance the transfer of properties from the filler to the polymer, and could result in improved performances and processing advantages.

Finally, the thermal stability of the composites with UTG (UTGO) was analyzed by TGA measurements (Figure 6 c, d). The temperature of maximum degradation rate of neat TPU is 351 °C. The presence of UTG in the TPU matrix leads to an increase by 9 ºC. No significant variation with the amount of UTG integrated in the TPU system is observed (Figure 6c). The addition of UTGO results in a slight increase of the temperature of maximum degradation rate compared with the composite with UTG (Figure 6d). Furthermore, a slower decomposition rate at temperature above 400°C is observed for the composite containing UTGO. At this temperature about 20 wt% less material is decomposed compared to the corresponding UTG composite. Thus, composite materials with higher thermal stability are produced by introduction of UTG or UTGO fillers, which both act as a barrier to delay the degradation of composites [16, 19]. The use of UTGO, leading to additional interactions with the TPU matrix, moderately enhances the thermal stability of the corresponding composite material.

4. CONCLUSIONS

Polyurethane composites with different UTG loadings, and with oxidized UTGO have been prepared by a facile solution mixing method followed by coagulation processing. FTIR and Raman spectroscopic analysis reveal the existence of interactions between the polymer and UTG, and these interactions intensify with increasing UTG content. A significant enhancement of the mechanical properties, resulting in an increase of more than 300% in the storage modulus for the composite with 3 wt% of UTG is observed, indicating a substantial reinforcing effect. Correspondingly, an increase in viscosity with UTG content achieving values 150 % higher for composites containing 3 wt% of UTG points to the effective formation of a UTG network in the TPU polymer matrix Furthermore, the presence of UTG significantly impacts on the thermal properties. Enhancement of the crystallization temperature by up to 30 ºC and increase of the thermal stability by 10 ºC for the composite with the highest UTG content of 3 wt% is achieved. UTGO containing TPU composites show a somewhat distinct behavior. Here, a reduction of the heat of fusion, i.e. the overall degree of crystallinity by 50 % compared to the neat TPU, is observed. This is accompanied by a significant, yet still moderate increase of the melting temperature by 2.5 ºC, indicative for somewhat larger crystallites present in the composites. Moreover, the thermal stability of the TPU-UTGO composite is 20% higher compared to the corresponding TPU-UTG composite. Most likely, the observed differences are a consequence of the presence of chemical interactions between oxygen functional groups and defects in UTGO material and the TPU polymer matrix. Summarizing, solution mixing applied to commercial UTG and TPU materials is a valuable strategy for fabricating corresponding TPU-UTG composites with substantially improved mechanical, thermal and processing characteristics. Controlling the degree of oxygen functional groups may be used to

14

further tailoring chemical interactions and the composites properties. The approach

presented is a straightforward proof of the value of already available commercial UTG

materials and is suitable for further industrial production.

5. ACKNOWLEDGMENTS

REFERENCES

[1] Paul DR, Robeson LM. Polymer nanotechnology: Nanocomposites. Polymer.

2008;49(15):3187-3204.

[2] Moniruzzaman M, Winey KI. Polymer nanocomposites containing carbon

nanotubes. Macromolecules. 2006;39(16):5194-5205.

[3] Winey KI, Vaia RA. Polymer Nanocomposites. MRS Bulletin. 2007;32:314-322.

[4] Geim AK, Novoselov KS. The rise of graphene. Nature Materials. 2007;6(3):183-

191.

[5] Geim AK. Graphene: Status and Prospects. Science. 2009;324(5934):1530-1534.

[6] Potts JR, Dreyer DR, Bielawski CW, Ruoff RS. Graphene-based polymer

nanocomposites. Polymer. 2011;52(1):5-25.

15

[7] Mukhopadhyay P, Gupta RK. Trends and Frontiers in Graphene-Based Polymer Nanocomposites. Plastics Engineering. 2011;1:32-42.

[8] Hepburn C. Polyurethane Elastomers. 2nd ed. New York, USA: Elsevier Applied Science; 1992.

[9] Oertel G. Polyurethane handbook. 2nd ed. Munich: Hanser Publishers; 1993.

[10] Xiong J, Zheng Z, Qin X, Li M, Li H, Wang X. The thermal and mechanical properties of a polyurethane/multi-walled carbon nanotube composite. Carbon. 2006;44(13):2701-2707.

[11] Sahoo NG, Jung YC, Yoo HJ, Cho JW. Effect of Functionalized Carbon Nanotubes on Molecular Interaction and Properties of Polyurethane Composites. Macromolecular Chemistry and Physics. 2006;207(19):1773-1780.

[12] Jana RN, Cho JW. Thermal stability and molecular interaction of polyurethane nanocomposites prepared by in situ polymerization with functionalized multiwalled carbon nanotubes. Journal of Applied Polymer Science. 2008;108(5):2857-2864.

[13] Khan U, Blighe FM, Coleman JN. Selective Mechanical Reinforcement of Thermoplastic Polyurethane by Targeted Insertion of Functionalized SWCNTs. The Journal of Physical Chemistry C. 2010;114(26):11401-11408.

[14] Fernández-d'Arlas B, Khan U, Rueda L, Coleman JN, Mondragon I, Corcuera MA, et al. Influence of hard segment content and nature on polyurethane/multiwalled carbon nanotube composites. Composites Science and Technology. 2011;71(8):1030-1038.

[15] Fernández M, Landa M, Muñoz ME, Santamaría A. Thermal and Viscoelastic Features of New Nanocomposites Based on a Hot-Melt Adhesive Polyurethane and Multi-Walled Carbon Nanotubes. Macromolecular Materials and Engineering. 2010;295(11):1031-1041.

[16] Pizzatto L, Lizot A, Fiorio R, Amorim CnL, Machado G, Giovanela M, et al. Synthesis and characterization of thermoplastic polyurethane/nanoclay composites. Materials Science and Engineering: C. 2009;29(2):474-478.

[17] Kim BK, Seo JW, Jeong HM. Morphology and properties of waterborne polyurethane/clay nanocomposites. European Polymer Journal. 2003;39(1):85-91.

[18] Wang Z, Pinnavaia TJ. Nanolayer Reinforcement of Elastomeric Polyurethane. Chem Mat. 1998;10(12):3769-3771.

[19] Lee YR, Raghu AV, Jeong HM, Kim BK. Properties of Waterborne Polyurethane/Functionalized Graphene Sheet Nanocomposites Prepared by an in situ Method. Macromolecular Chemistry and Physics. 2009;210(15):1247-1254.

[20] Khan U, May P, O'Neill A, Coleman JN. Development of stiff, strong, yet tough composites by the addition of solvent exfoliated graphene to polyurethane. Carbon. 2010;48(14):4035-4041.

[21] Nguyen DA, Lee YR, Raghu AV, Jeong HM, Shin CM, Kim BK. Morphological and physical properties of a thermoplastic polyurethane reinforced with functionalized graphene sheet. Polymer International. 2009;58(4):412-417.

[22] Yoon S, Park J, Kim E, Kim B. Preparations and properties of waterborne polyurethane/allyl isocyanated-modified graphene oxide nanocomposites. Colloid & Polymer Science. 2011;289(17):1809-1814.

[23] Choi J, Kim D, Ryu K, Lee H-i, Jeong H, Shin C, et al. Functionalized graphene sheet/polyurethane nanocomposites: Effect of particle size on physical properties. Macromolecular Research. 2011;19(8):809-814.

[24] Cai D, Yusoh K, Song M. The mechanical properties and morphology of a graphite oxide nanoplatelet/polyurethane composite. Nanotechnology. 2009;20(8):085712.

17

[25] Kim H, Miura Y, Macosko CW. Graphene/Polyurethane Nanocomposites for Improved Gas Barrier and Electrical Conductivity. Chem Mat. 2010;22(11):3441-3450.

[26] Naeimi H, Mohajeri A, Moradi L, Rashidi AM. Efficient and facile one pot carboxylation of multiwalled carbon nanotubes by using oxidation with ozone under mild conditions. Applied Surface Science. 2009;256(3):631-635.

[27] Ferrari AC. Raman spectroscopy of graphene and graphite: diorder, electron-phonon coupling, doping and nonadiabatic effects. Solid State Communications. 2007;143(1-2):47-57.

[28] Mishra AK, Chattopadhyay DK, Sreedhar B, Raju KVSN. FT-IR and XPS studies of polyurethane-urea-imide coatings. Progress in Organic Coatings. 2006;55(3):231-243.

[29] Chen X, Chen X, Lin M, Zhong W, Chen X, Chen Z. Functionalized Multi-Walled Carbon Nanotubes Prepared by In Situ Polycondensation of Polyurethane. Macromolecular Chemistry and Physics. 2007;208(9):964-972.

[30] Gong L, Kinloch IA, Young RJ, Riaz I, Jalil R, Novoselov KS. Interfacial Stress Transfer in a Graphene Monolayer Nanocomposite. Advanced Materials. 2010;22(24):2694-2697.

[31] Sperling LH. Introduction to Physical Polymer Science. 3rd ed. New York: Wiley-Interscience; 2001.

[32] Metzger TG. The Rheology Handbook: Vincentz Verlag; 2006.

[33] Huang YY, Ahir SV, Terentjev EM. Dispersion rheology of carbon nanotubes in a polymer matrix. Physical Review B. 2006;73(12):125422-125430.

[34] Abdel-Goad M, Pötschke P. Rheological characterization of melt processed polycarbonate-multiwalled carbon nanotube composites. Journal of Non-Newtonian Fluid Mechanics. 2005;128(1):2-6.
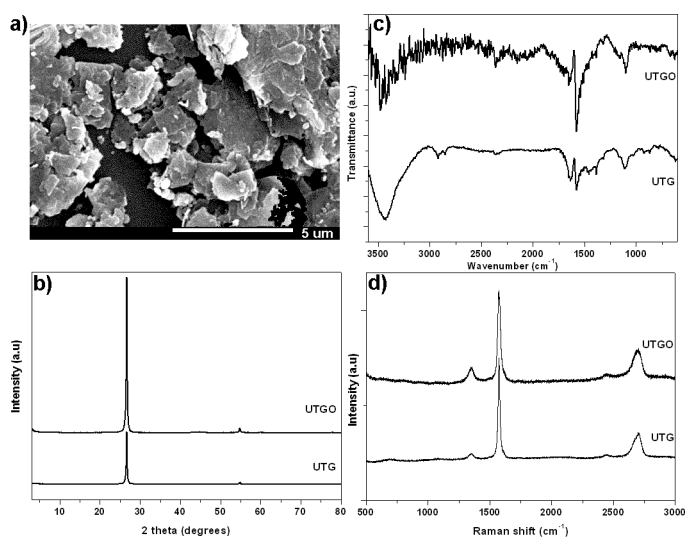
FIGURES

Figure 1. SEM micrograph of UTG (a), X-Ray diffractograms (b), FTIR (c), and
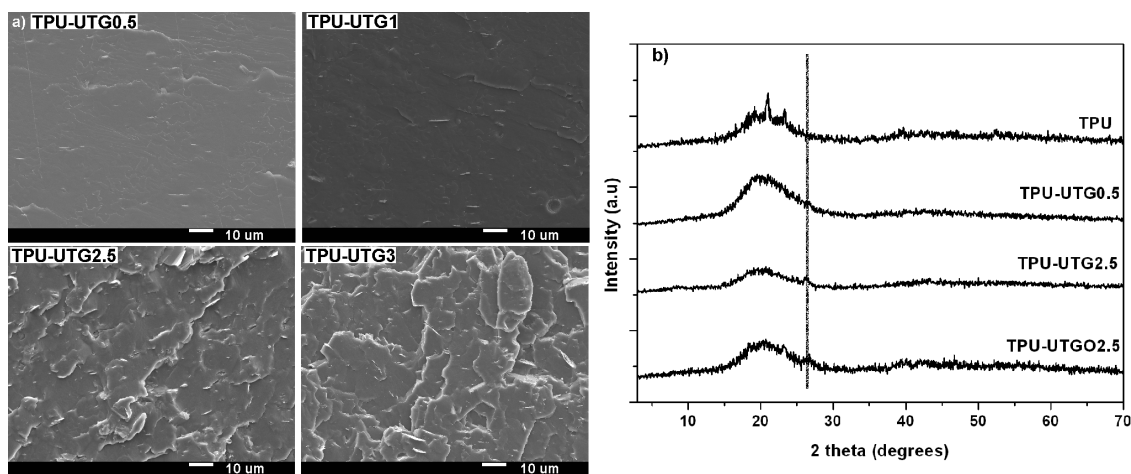
Raman spectra (d) of UTG and UTGO.

Figure 2. FE-SEM micrographs (cross-sectional fracture) (a), and X-ray diffractograms

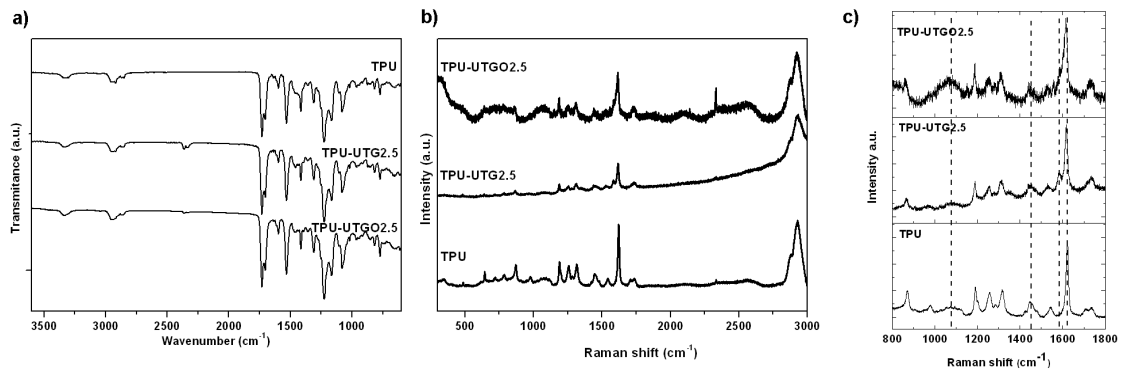(b) of TPU-UTG(O) composites. Line in (b) indicates position of graphite (002) peak.

19

Figure 3. FTIR (a) and Raman (b, c) spectra of neat TPU, TPU-UTG and TPU-UTGO composites. Details of Raman bands are depicted in (c).
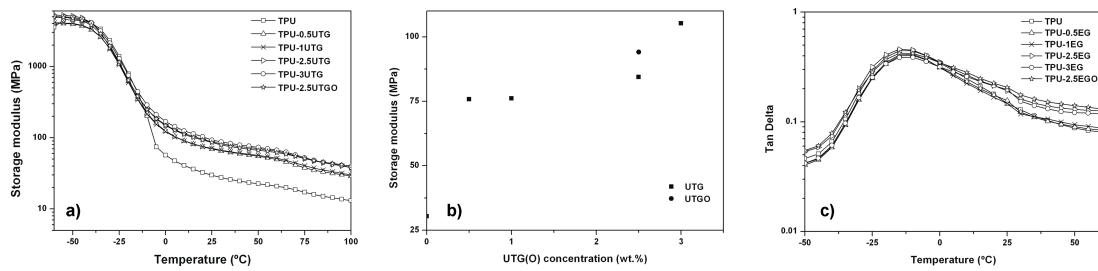

Figure 4. DMA curves of TPU, TPU-UTG and TPU-UTGO composites. Storage modulus E' (a), E'$_{max}$ (RT) as a function of UTG(O) concentration and tan δ curve (c).
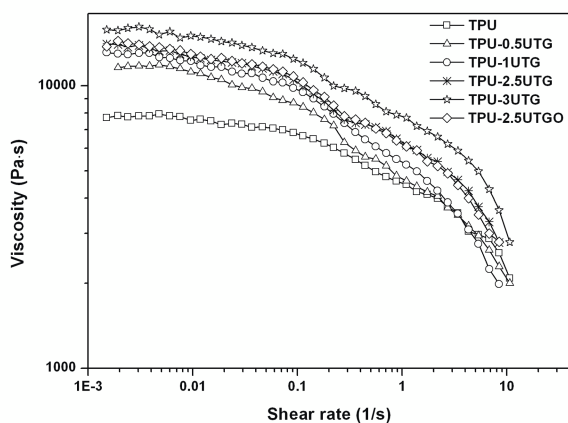
Figure 5. Rheological analysis showing the viscosity behavior of neat TPU, TPU-UTG and TPU-UTGO composites.
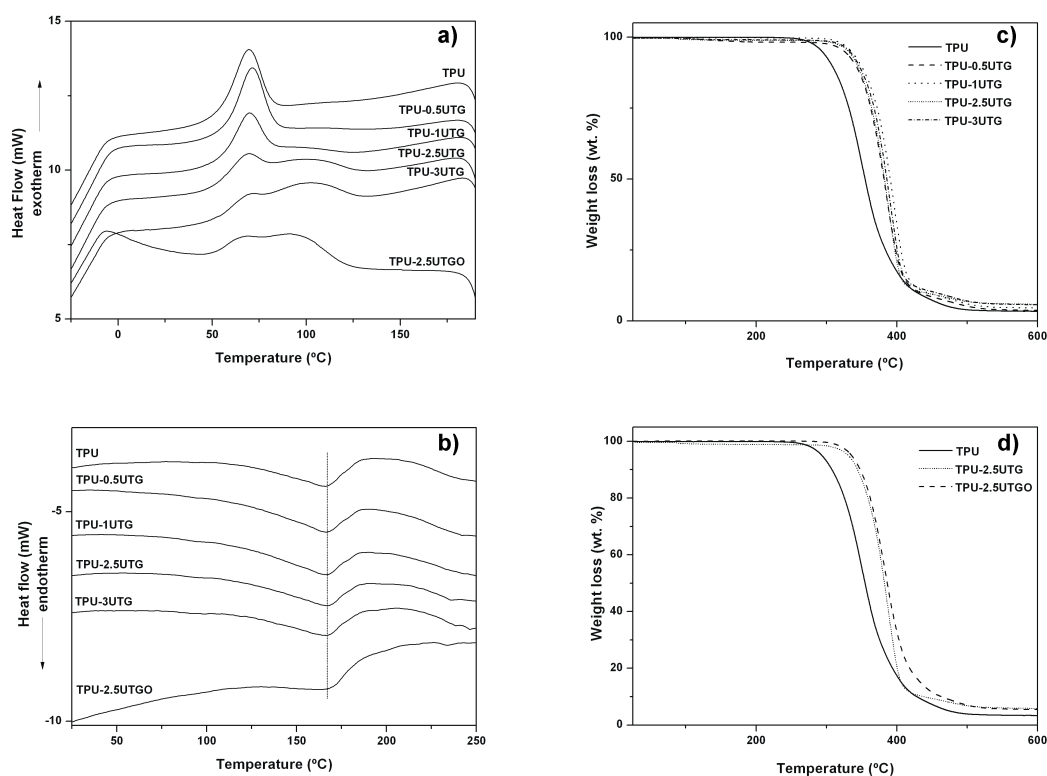

Figure 6. DSC and TGA curves of TPU, TPU-UTG and TPU-UTGO composites. DSC crystallization curves (a), DSC melting curves (b), TGA (c), direct comparison of TPU, TPU-UTG2.5 and TPU-UTGO2.5 composites. Line in (b) indicates the position of the melting temperature of TPU.

TABLES

Table 1. Values for glass transition temperature T_g, melting temperature T_m and heat of

fusion ΔH_m for neat TPU, TPU-UTG and TPU-UTGO composites.

Material	T_g (ºC)*	T_m (ºC)**	ΔH_m (J/g)**
TPU	-18.04	165.96	-7.32
TPU-0.5UTG	-17.03	166.24	-7.11
TPU-1UTG	-14.01	166.75	-7.10
TPU-2.5UTG	-13,34	166.77	-6.96
TPU-3UTG	-12.59	166.79	-6.17
TPU-2.5UTGO	-13.24	168.42	-3.23

* Derived from maximum of tan δ curve. ** Derived from DSC melting curve.